

EVALUATION OF EFFECTIVE MATERIAL PROPERTIES OF THICKNESS-SHEAR PIEZOELECTRIC MACRO-FIBRE COMPOSITES

Marcelo Areias Trindade, trindade@sc.usp.br

Department of Mechanical Engineering, São Carlos School of Engineering, University of São Paulo, São Carlos, SP, 13566-590, Brazil

Ayech Benjeddou, benjeddou@supmeca.fr

Institut Supérieur de Mécanique de Paris, LISMMA/Structures, 3 rue Fernand Hainault, 93407 Saint Ouen, France

Abstract. A finite element homogenization method for a shear actuated d_{15} Macro-Fibre Composite (MFC) made of seven layers (Kapton, Acrylic, Electrode, Piezoceramic Fibre and Epoxy Composite, Electrode, Acrylic, Kapton) is proposed and used for the characterization of its effective material properties. The methodology was already validated for the MFC active layer only, made of piezoceramic fibre and epoxy, through comparison with analytical results. Its use for the analysis of full seven-layers MFCs has shown that the packaging reduces significantly the shear stiffness of the transducer and, thus, leading to significantly smaller effective electromechanical coupling coefficient k_{15} and piezoelectric stress constant e_{15} when compared to the piezoceramic fibre properties. However, it was found that the piezoelectric charge constant d_{15} is less affected by the softer layers required by the MFC packaging. As an extension of this previous study, this work presents a parametric analysis for which fibre volume fraction, Epoxy elastic modulus and electrode thickness are varied. Results show that both fibre volume fraction and Epoxy elastic modulus affect significantly the electromechanical coupling coefficient of the proposed MFC and, thus, its performance as sensor, actuator and energy converter.

Keywords: Macro-fibre composites, shear actuators, properties characterization, finite element homogenization method

1. INTRODUCTION

Recent applications of piezoelectric sensors and actuators require conformability and packaging standards not found in monolithic piezoceramic patches. The so-called Macro-Fibre Composites (MFC) have become very popular since they combine the conformability of epoxy-matrix composites and the electromechanical energy density of piezoceramic materials (Wilkie *et al.*, 2000). The concept is based on Piezoelectric Fibre Composites (PFC) proposed before (Bent and Hagood, 1997) that used extruded piezoceramic fibres (circular cross-section) embedded to an epoxy-based resin matrix and covered by Copper electrodes and protective Kapton and/or Acrylic layers. However, the MFCs replace the extruded piezoceramic fibres by machined (diced) rectangular fibres of a piezoceramic material. This innovation led to a cheaper and more reliable manufacturing process and allowed direct contact between fibres and electrodes, solving the main problem of permittivity mismatch of PFCs. The original MFC idea developed at NASA (Wilkie *et al.*, 2000) uses Interdigitated Electrodes (IDE) to induce longitudinal or 33 mode in the fibres. But, nowadays, it is possible to find MFCs using uniform field (continuous) electrodes that operate with the transverse or 31 mode in the fibres.

More recently, an alternative MFC design, in which the macro-fibres are oriented perpendicular to the direction of motion, was proposed (Raja and Ikeda, 2008) to induce the transverse shear mode (15 or 35) in the piezoceramic fibres. The transverse shear mode, or thickness shear mode, of piezoceramic materials can be obtained by the application of an electric field that is perpendicular to the remanent polarization direction. This leads to a rotation of the electrical dipoles which induces shear stresses/strains in the material. The transverse shear mode in commercially available piezoceramic patches is normally obtained by polarization along the length or width direction followed by removal of the electrodes used for polarization and deposition of new electrodes on the top and bottom surfaces. The presence of the new electrodes imposes a dominant electric field, either applied or induced, in the thickness direction, thus perpendicular to the length or width poling direction. Since the mid-90s, the shear mode of monolithic piezoceramic materials has been considered for applications in the design of smart structures (Benjeddou, 2007; Trindade and Benjeddou, 2009), including active (Raja *et al.*, 2002; Baillargeon and Vel, 2005) and passive (Benjeddou and Ranger, 2006; Trindade and Maio, 2008) vibration control. From these studies, the shear mode seems to be an interesting alternative for stiffer structures, higher frequencies and non-standard shape deflection patterns.

The main difficulty in the study of MFCs, as an alternative to monolithic piezoceramic patches, is that their behaviour may be much more complex since they are made of several different materials (piezoceramic fibres, epoxy matrix, electrode layers and protective layers). Therefore, it is necessary to understand and model their behaviour to be able to quantify or characterize their effective material properties and, thus, their effectiveness as distributed sensors and actuators. Recently, some research effort has been directed to the identification and characterization of such transducers, in extension (33 or 31) (Deraemaeker *et al.*, 2009) and transverse shear (15) (Benjeddou and Al-Ajmi, 2009) modes. It has been shown that the effective properties depend not only on the piezoceramic material used for the fibres and epoxy material used for the matrix and epoxy-to-piezoceramic volume fraction but also on the geometrical and material properties of the other layers (Kapton, Acrylic, Electrodes). Some analytical methods from the composite materials literature, such as the Asymptotic Homogenization Method (AHM) (Benjeddou and Al-Ajmi, 2009; Otero *et al.*, 2005) and the Uniform Field Method (UFM) (Bent and Hagood, 1997), can be applied to obtain the effective properties of the composite transducer

from the properties of its components. Alternatively, one may use techniques based on finite element modelling of the composite transducer to identify its effective properties (Berger *et al.*, 2005).

A previous study of a shear actuated d_{15} MFC made of seven layers (Kapton, Acrylic, Electrode, Piezoceramic Fibre and Epoxy Composite, Electrode, Acrylic, Kapton) using a finite element homogenization method to characterize its effective material properties was presented in (Trindade and Benjeddou, 2010). It has shown that the packaging reduces significantly the shear stiffness of the piezoceramic material and, thus, leading to significantly smaller effective electromechanical coupling coefficient k_{15} and piezoelectric stress constant e_{15} when compared to the piezoceramic fibre properties. However, it was found that the piezoelectric charge constant d_{15} is less affected by the softer layers required by the MFC packaging. This work presents, first, an analysis similar to the previous one (Trindade and Benjeddou, 2010) but using another electrode design and, second, a parametric analysis in which the effect of the variations of fibre volume fraction, Epoxy elastic modulus and electrode thickness on the effective material properties is evaluated.

2. MACRO-FIBRE COMPOSITES

Macro-Fibre Composites (MFCs) that are commercially available use either the 33 or 31 response modes, meaning that the piezoelectric constant that characterizes their actuation/sensing behaviour is respectively the d_{33} or d_{31} , and therefore are named as d_{33} or d_{31} MFCs. Schematic representations of the d_{33} and d_{31} MFCs are shown in Figures 1 and 2, respectively. The major differences between the two commercially available MFCs are the electrode design and the poling direction of the fibres. In the d_{31} MFC, the poling direction is perpendicular to the fibres (along their thickness) so that transverse extension of the fibres can be obtained through the d_{31} constant. On the other hand, in the d_{33} MFC, the poling direction follows a complex non uniform distribution according to the disposition of the interdigitated positive and negative electrodes (IDE) aiming to yield an equivalent macroscopic poling direction parallel to the fibre length, so that longitudinal extension of the fibres can be obtained through the d_{33} constant. The main problem of the d_{33} MFC is that the equivalent macroscopic longitudinal poling direction, and thus its performance, increases with the distance between interdigitated electrode fingers which leads to the requirement of a high actuation voltage (up to 1200 V) to generate the necessary electric field. The d_{31} MFC, on the other hand, requires much lower actuation voltages since the electric field is uniform and in the direction of the actuator thickness, which can be made quite small, but its piezoelectric constant d_{31} is much smaller than d_{33} .

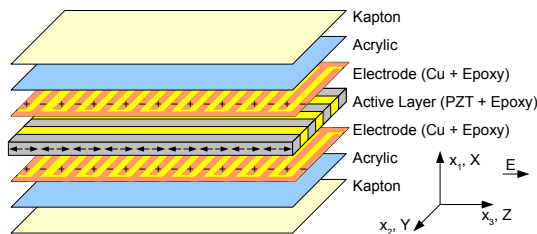


Figure 1. Schematic representation of longitudinal “ d_{33} ” Macro-Fibre Composite.

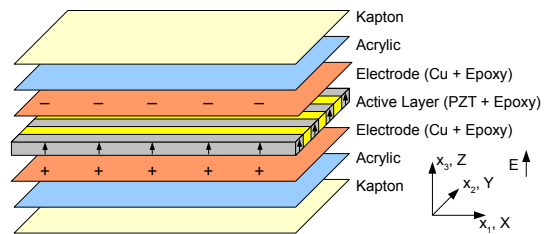


Figure 2. Schematic representation of transverse “ d_{31} ” Macro-Fibre Composite.

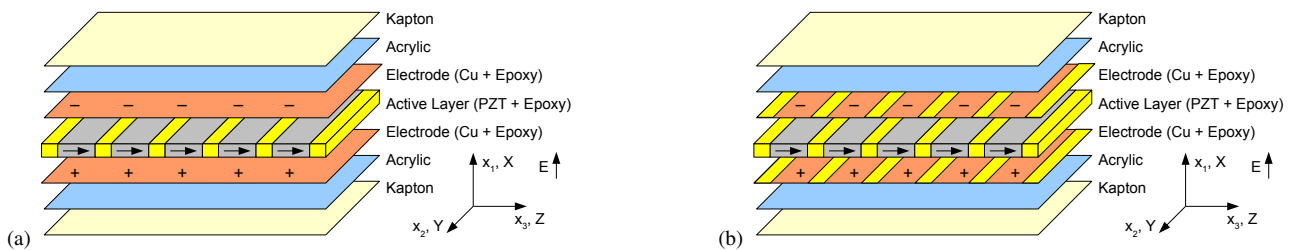


Figure 3. Schematic representations of thickness-shear “ d_{15} ” Macro-Fibre Composite with (a) continuous or homogeneous electrodes and (b) discontinuous or heterogeneous electrodes.

The motivations for the development of a d_{15} MFC is to take advantage of the high piezoelectric coupling constant d_{15} that most piezoceramic materials have and the fact that it couples directly to transverse shear strains. The first concept of a d_{15} MFC was recently presented by Raja and Ikeda (Raja and Ikeda, 2008), named as Shear Actuated Fibre Composite (SAFC) by the authors, taking advantage of the known fabrication procedures of the d_{31} and d_{33} MFCs. It basically consists of piezoceramic fibres with poling direction perpendicular to the fibre longitudinal axis, as for the d_{33} MFC, but instead of orienting the fibres along the longitudinal direction of the actuator, as for the d_{33} MFC, the fibres are oriented along the width of the actuator so that poling direction is in the longitudinal direction of the actuator, as shown in Figure 3. Different from the IDE proposition of (Raja and Ikeda, 2008), a continuous (Figure 3a) or woven-type (Figure 3b)

electrode, such as those used in commercial d_{31} MFCs, can be used to induce a uniform electric field in direction of the actuator thickness (Benjeddou and Al-Ajmi, 2009; Trindade and Benjeddou, 2010). As the fibres are poled in their width direction, that is the longitudinal direction of the actuator, a shear strain is induced in the fibres transversal planes. The width-poled piezoceramic fibers can be made by dice cutting either thickness-poled or longitudinal- or width-poled piezoceramic plates. However, in the first case, proposed by (Raja and Ikeda, 2008), the resulting fibres should be rotated 90° around their axes before positioning them in the Epoxy-Copper electrode layer, so that the poling direction of each fibre coincides with the longitudinal direction of the actuator, which can be difficult in practice. In the second case, several width-poled plates can be aligned in the polymer film frame before dice cutting of the ensemble leading to a probably cheaper process to produce aligned fibres poled in the width direction, which after packaging would be the longitudinal direction of the actuator.

3. CONSTITUTIVE EQUATIONS FOR SHEAR PIEZOELECTRIC MATERIALS

The shear or d_{15} response mode requires that poling vector P and main electric field E to be perpendicular to each other. From the modelling point of view, this can be achieved, in one way as in Figure 3, by positioning reference axes such that the poling direction, width of fibre or length of actuator, coincides with direction x_3 or z and the fibre thickness, and actuator thickness, coincides with direction x_1 or x . The other way to achieve d_{15} mode would be to orient the fibre thickness in x_3 direction and the fibre width and poling in x_1 direction. The latter has the advantage to use the axes orientation standard to the analysis of thin plates but requires a 90° rotation around x_2 direction of the standard constitutive equations for piezoelectric materials poled in x_3 direction. Therefore, for the present work, the former (as in Figure 3) was used to provide easier results interpretation as compared to commercial MFCs and standard piezoelectricity notation.

Starting from the electric enthalpy for a linear orthotropic piezoelectric material poled in x_3 direction and considering that electrodes fully cover top (x_1^+) and bottom (x_1^-) surfaces such that a preferential or dominant x_1 direction is imposed for the electric field and displacement, such that $E_2 = E_3 = 0$ or $D_2 = D_3 = 0$, the constitutive equations can be written in a mixed type form, so-called e -form, as

$$\begin{pmatrix} T_1 \\ T_2 \\ T_3 \\ T_4 \\ T_5 \\ T_6 \\ D_1 \end{pmatrix} = \begin{bmatrix} c_{11}^E & c_{12}^E & c_{13}^E & 0 & 0 & 0 & 0 \\ c_{12}^E & c_{22}^E & c_{23}^E & 0 & 0 & 0 & 0 \\ c_{13}^E & c_{23}^E & c_{33}^E & 0 & 0 & 0 & 0 \\ 0 & 0 & 0 & c_{44}^E & 0 & 0 & 0 \\ 0 & 0 & 0 & 0 & c_{55}^E & 0 & -e_{15} \\ 0 & 0 & 0 & 0 & 0 & c_{66}^E & 0 \\ \hline 0 & 0 & 0 & 0 & e_{15} & 0 & \epsilon_{11}^S \end{bmatrix} \begin{pmatrix} S_1 \\ S_2 \\ S_3 \\ S_4 \\ S_5 \\ S_6 \\ E_1 \end{pmatrix}. \quad (1)$$

where T_p and S_q , with $p, q = 1, \dots, 6$, denote the six components of mechanical stress and strain in Voigt notation. D_i and E_k , with $i, k = 1, 2, 3$, denote the three components of electric displacement and field. c_{pq}^E , e_{kp} and ϵ_{ik}^S denote the elastic stiffness (at constant electric fields), piezoelectric and electric permittivity (at constant mechanical strains) constants.

The main electromechanical coupling is between the electric field and displacement in x_1 direction, E_1 and D_1 , and $x_1 - x_3$ shear stress and strain, T_5 and S_5 . Thus, this is known as '15' operation mode. The electromechanical coupling coefficient can be defined from the value of the coupling or interaction coefficient relative to the principal or diagonal coefficients (Ikeda, 1990) using the standard intensive type or d -form of the constitutive equations, such that

$$k_{15}^2 = \frac{d_{15}^2}{s_{55}^E \epsilon_{11}^T} \text{ where } d_{15} = e_{15}/c_{55}^E, s_{55}^E = 1/c_{55}^E \text{ and } \epsilon_{11}^T = \epsilon_{11}^S/(1 - k_{15}^2). \quad (2)$$

This expression can be also written in terms of the e_{15} constant present in the e -form of the constitutive equations or using the relations between the constants appearing in different forms of the constitutive equations such as

$$k_{15}^2 = \frac{e_{15}^2}{c_{55}^E \epsilon_{11}^T} = \frac{e_{15}^2}{c_{55}^D \epsilon_{11}^S} = 1 - c_{55}^E/c_{55}^D = 1 - \epsilon_{11}^S/\epsilon_{11}^T. \quad (3)$$

It is thus clear that the material properties d_{15} , c_{55}^E and ϵ_{11}^T are of major importance for the evaluation of the potential of such material as a candidate for the development of transducers (actuators and sensors). The Table 1 presents typical values of these constants for a number of commercially available piezoceramic materials.

In the case of d_{15} MFCs which are composed of a number of materials, it is important to identify the effective properties of the ensemble based on its constituents properties. For that, the Representative Volume Element (RVE) technique together with Ansys^(R) finite element software is used to evaluate effective material properties of multilayer d_{15} MFCs.

4. FINITE ELEMENT NUMERICAL HOMOGENIZATION

In this section, a numerical homogenization using the finite element method is applied to evaluate the effective properties of a d_{15} MFC including the electrode and protective layers, according to the schematic representation of Figure

Table 1. Shear mode d_{15} properties of some commercially available piezoceramic materials.

	c_{55}^E (GPa)	$\epsilon_{11}^T/\epsilon_0$	d_{15} (pC/N)	e_{15} (C/m ²)	k_{15}^2 (%)	k_{15} (%)
APC-840	26.9	1427	480	13.6	49.0	70
APC-850	21.8	1851	590	13.2	46.2	68
APC-855	22.4	3012	720	15.0	43.6	66
EC-76	21.9	2853	730	16.0	46.2	68
EC-64	25.7	1436	506	13.0	51.8	72
PIC-255	21.0	1650	550	11.6	43.6	66
PZT-5H	23.0	3130	740	17.0	45.6	68
PZT-5A	21.1	1730	584	12.3	46.9	68
PZT-7A	29.4	930	360	10.6	46.2	68
Sonox-P502	30.1	1950	560	16.9	54.8	74
Sonox-P504	24.8	1920	530	13.2	43.6	66
Sonox-P508	29.8	1700	550	16.4	50.4	71

3b (Berger *et al.*, 2005; Deraemaeker *et al.*, 2007; Trindade and Benjeddou, 2010). It consists in imposing mechanical displacement and force boundary conditions on the boundaries of the RVE ($X_1^-, X_1^+, X_2^-, X_2^+, X_3^-, X_3^+$). In addition, electric boundary conditions are imposed at the electrodes on surfaces X_1^{e-} and X_1^{e+} . In case of the RVE considered for the d_{15} MFC, shown in Figure 4, these boundaries are $X_1^-: x_1 = 0, X_1^+: x_1 = h_P + 2(h_E + h_A + h_K), X_2^-: x_2 = 0, X_2^+: x_2 = w, X_3^-: x_3 = 0, X_3^+: x_3 = L_P + L_E, X_1^{e-}: x_1 = h_E + h_A + h_K, X_1^{e+}: x_1 = h_P + h_E + h_A + h_K$.

The protective layers, made of Kapton and Acrylic materials, and electrode layer, made of Copper and Epoxy, are considered isotropic. As the active layer is orthotropic, the d_{15} MFC composed of seven layers Kapton / Acrylic / Cu+Epoxy / PZT+Epoxy / Cu+Epoxy / Acrylic / Kapton should also be orthotropic. Therefore, the finite element homogenization method considered for the active layer could be also applied to the 7-layered d_{15} MFC. Notice that the isotropy of the electrode layer depends on its design. Electrode designs such as those used for d_{31} MFC (continuous or woven-type) seem to be more reasonable than those used for the d_{33} MFC (interdigitated) since the voltage should ideally be constant all over the fibre surfaces. An isotropic continuous electrode (Figure 3a) was considered in a previous work (Trindade and Benjeddou, 2010) but, in this work, a discontinuous electrode (Epoxy/Copper/Epoxy) is considered (Figure 3b).

Average strains and electric fields can therefore be imposed to the RVE using displacements and voltage boundary conditions, such that

$$u_i^{X_j^+} - u_i^{X_j^-} = \bar{S}_{ij}(x_j^{X_j^+} - x_j^{X_j^-}), \quad i, j = 1, 2, 3, \quad (4)$$

and

$$\phi^{X_1^{e+}} - \phi^{X_1^{e-}} = \bar{E}_1(x_1^{X_1^{e+}} - x_1^{X_1^{e-}}). \quad (5)$$

The resulting average strains, stresses, electric fields and electric displacements in the RVE are defined as

$$\bar{S}_q = \frac{1}{V} \int_V S_q \, dV, \quad \text{and} \quad \bar{T}_p = \frac{1}{V} \int_V T_p \, dV, \quad \text{with} \quad p, q = 1, \dots, 6, \quad (6)$$

$$\bar{E}_k = \frac{1}{V} \int_V E_k \, dV, \quad \text{and} \quad \bar{D}_i = \frac{1}{V} \int_V D_i \, dV, \quad \text{with} \quad i, k = 1, 2, 3. \quad (7)$$

These integrals are approximated in Ansys^(R) by a sum over averaged element values multiplied by the respective element volume divided by total volume of the RVE, such that

$$\bar{S}_q = \frac{\sum_{e=1}^N S_q^{(e)} V^{(e)}}{\sum_{e=1}^N V^{(e)}}, \quad \text{and} \quad \bar{T}_p = \frac{\sum_{e=1}^N T_p^{(e)} V^{(e)}}{\sum_{e=1}^N V^{(e)}}, \quad \text{with} \quad p, q = 1, \dots, 6, \quad (8)$$

$$\bar{E}_k = \frac{\sum_{e=1}^N E_k^{(e)} V^{(e)}}{\sum_{e=1}^N V^{(e)}}, \quad \text{and} \quad \bar{D}_i = \frac{\sum_{e=1}^N D_i^{(e)} V^{(e)}}{\sum_{e=1}^N V^{(e)}}, \quad \text{with} \quad i, k = 1, 2, 3. \quad (9)$$

where $V^{(e)}$ is the volume of the element e . $S_q^{(e)}$, $T_p^{(e)}$, $E_k^{(e)}$ and $D_i^{(e)}$ are the average strains, stresses, electric fields and electric displacements evaluated at element e . N is the total number of finite elements used to discretize the RVE.

For the evaluation of the elastic constants c_{pq}^E , $p, q = 1, 2, 3$, related to normal strains and stresses, three local problems are analysed for which a normal strain S_q ($q = 1, 2, 3$) is applied by imposing normal displacements $u_q^{X_q^+}$ at surface X_q^+ while the normal displacements at all other surfaces are set to zero. This is done to obtain $\bar{S}_j = 0$ if $j \neq q$. To ensure a short

circuit electric boundary condition, the voltage degrees of freedom in the electrodes at surfaces X_1^{e-} and X_1^{e+} are set to zero. Then, considering the constitutive equations in (1), the effective elastic constants are evaluated using the following expressions

$$c_{pq}^E = \bar{T}_p / \bar{S}_q, \quad p, q, = 1, 2, 3, \quad (10)$$

where the average stresses \bar{T}_p and strains \bar{S}_q are evaluated using (8).

For the evaluation of the elastic constants related to shear strains and stresses c_{pp}^E , $p = 4, 5, 6$, other three local problems are analysed for which shear strains S_{ik} ($S_{23} = S_4/2$, $S_{13} = S_5/2$ and $S_{12} = S_6/2$) are applied to approximate a pure shear stress state in the planes $x_2 - x_3$, $x_1 - x_3$ and $x_1 - x_2$ by imposing shear displacements $u_i^{X_k^+}$ and $-u_i^{X_k^-}$ at surfaces X_k^+ and X_k^- and $u_k^{X_i^+}$ and $-u_k^{X_i^-}$ at surfaces X_i^+ and X_i^- . Moreover, the normal displacements at the boundary surfaces parallel to each shear plane of interest are set to zero to ensure zero strains perpendicular to the shear plane. To ensure a short circuit electric boundary condition, the voltage degrees of freedom in the electrodes at surfaces X_1^{e-} and X_1^{e+} are set to zero. Therefore, the effective elastic constants are evaluated in terms of the average shear stresses \bar{T}_p and strains \bar{S}_p using

$$c_{pp}^E = \bar{T}_p / \bar{S}_p, \quad p = 4, 5, 6. \quad (11)$$

The piezoelectric constant e_{15} can be also obtained from the local problem used to evaluate c_{55}^E , that is where a pure shear stress state in the plane $x_1 - x_3$ is approximated. From the constitutive equations (1), e_{15} can be obtained by evaluating the average electric displacement \bar{D}_1 such that

$$e_{15} = \bar{D}_1 / \bar{S}_5. \quad (12)$$

where the average shear strain \bar{S}_5 and electric displacement \bar{D}_1 are evaluated using the approximation of (8) and (9).

For the evaluation of the piezoelectric and dielectric constants of the d -form, d_{15} and ϵ_{11}^T , another local problem is set up for which an electric voltage $\phi^{X_1^{e+}} = h_P$ (in value) is applied to the electrode at surface X_1^{e+} ($x_1 = h_P + h_E + h_A + h_K$) while the voltage at the opposite electrode (at surface X_1^{e-} , $x_1 = h_E + h_A + h_K$) is set to zero so that a unitary electric field in the x_1 direction is generated. To approximate the condition of zero stresses in the RVE, no restriction is made to the displacements in the RVE except for the origin where all displacements are set to zero to prevent rigid body displacements. Then, considering zero shear stress T_5 in the d -form of the constitutive equations, the piezoelectric and dielectric constants, d_{15} and ϵ_{11}^T , can be evaluated from

$$d_{15} = \bar{S}_5 / \bar{E}_1 \text{ and } \epsilon_{11}^T = \bar{D}_1 / \bar{E}_1. \quad (13)$$

For the evaluation of the blocked dielectric constant ϵ_{11}^S , an electric voltage $\phi^{X_1^{e+}} = h_P$ (in value) is applied to the electrode at surface X_1^{e+} while the voltage at the opposite electrode (X_1^{e-}) is set to zero so that a unitary electric field in the x_1 direction is generated. To approximate the condition of zero strains in the RVE, the displacements at all six surfaces of the RVE are set to zero. Hence, from the constitutive equations (1), the dielectric constant ϵ_{11}^S can be evaluated from

$$\epsilon_{11}^S = \bar{D}_1 / \bar{E}_1, \quad (14)$$

where \bar{D}_1 and \bar{E}_1 are evaluated using the approximation of (9). Table 2 summarizes the local problems used for the characterization of relevant d_{15} MFC material properties.

5. d_{15} MFC EFFECTIVE MATERIAL PROPERTIES

Figure 5 shows the finite element mesh used in Ansys^(R) for the 7-layered d_{15} MFC RVE using a FVF of 0.86 for the PZT+Epoxy Active Layer. The 3D 20-Node coupled-field solid finite element SOLID226 was used to mesh all volumes. 5525 finite elements were used considering 25 divisions in x_1 direction (13 divisions for the PZT layer and 2 divisions for each electrode and protective layer), 13 divisions in x_2 direction and 17 divisions in x_3 direction (11 divisions for the PZT layer and 3 divisions for each Epoxy layer). According to Figure 4, the dimensions considered for this RVE are $h_P = 1$ mm, $h_K = 25.4$ μ m, $h_A = 12.7$ μ m and $h_E = 17.8$ μ m, $L_P = 0.860$ mm, $L_E = 0.140$ mm and $w = 1$ mm (Raja and Ikeda, 2008). The material properties for the piezoceramic material Sonox P502, taken from Deraemaeker *et al.* (2009), are: $s_{11}^E = s_{22}^E = 18.5$ pm²/N, $s_{33}^E = 20.7$ pm²/N, $s_{12}^E = -6.29$ pm²/N, $s_{13}^E = -6.23$ pm²/N, $s_{44}^E = s_{55}^E = 33.2$ pm²/N, $s_{66}^E = 52.3$ pm²/N, $d_{31} = d_{32} = -185$ pC/N, $d_{33} = 440$ pC/N, $d_{15} = d_{24} = 560$ pC/N, $\epsilon_{11}^T = \epsilon_{22}^T = 1950\epsilon_0$, $\epsilon_{33}^T = 1850\epsilon_0$. The material properties for the isotropic Epoxy are: $Y = 2.9$ GPa, $\nu = 0.3$ and $\epsilon = 4.25\epsilon_0$. The materials properties for the protective layers, taken from (Raja and Ikeda, 2008), are: Kapton - $Y = 2.5$ GPa, $\nu = 0.34$ and $\epsilon = 3.4\epsilon_0$ and Acrylic - $Y = 2.7$ GPa, $\nu = 0.35$ and $\epsilon = 3.4\epsilon_0$. The material properties for the Copper electrode are: $Y = 117$ GPa, $\nu = 0.35$ and $\epsilon = 5\epsilon_0$.

Table 2. Boundary conditions and relations used to evaluate effective material properties of d_{15} piezoelectric MFC.

Problem	Constant	Displacements						Potential		Relation	Expression
		X_1^-	X_1^+	X_2^-	X_2^+	X_3^-	X_3^+	X_1^{e-}	X_1^{e+}		
1	c_{11}^E	0	u_1	0	0	0	0	0	0	\bar{T}_1/\bar{S}_1	(10)
1	c_{12}^E	0	u_1	0	0	0	0	0	0	\bar{T}_2/\bar{S}_1	(10)
1	c_{13}^E	0	u_1	0	0	0	0	0	0	\bar{T}_3/\bar{S}_1	(10)
2	c_{22}^E	0	0	0	u_2	0	0	0	0	\bar{T}_2/\bar{S}_2	(10)
2	c_{23}^E	0	0	0	u_2	0	0	0	0	\bar{T}_3/\bar{S}_2	(10)
3	c_{33}^E	0	0	0	0	0	u_3	0	0	\bar{T}_3/\bar{S}_3	(10)
4	c_{44}^E	0	0	$-u_3$	u_3	$-u_2$	u_2	0	0	\bar{T}_4/\bar{S}_4	(11)
5	c_{55}^E	$-u_3$	u_3	0	0	$-u_1$	u_1	0	0	\bar{T}_5/\bar{S}_5	(11)
5	e_{15}	$-u_3$	u_3	0	0	$-u_1$	u_1	0	0	\bar{D}_1/\bar{S}_5	(12)
6	c_{66}^E	$-u_2$	u_2	$-u_1$	u_1	0	0	0	0	\bar{T}_6/\bar{S}_6	(11)
7	d_{15}	-	-	-	-	-	-	0	ϕ	\bar{S}_5/\bar{E}_1	(13)
7	ϵ_{11}^T	-	-	-	-	-	-	0	ϕ	\bar{D}_1/\bar{E}_1	(13)
8	ϵ_{11}^S	0	0	0	0	0	0	0	ϕ	\bar{D}_1/\bar{E}_1	(14)

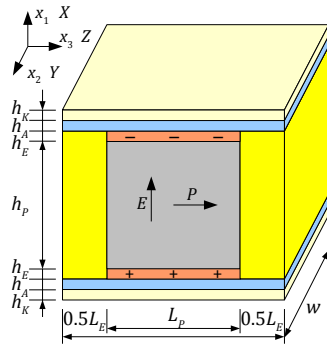


Figure 4. Representative volume element (RVE) for a d_{15} MFC.

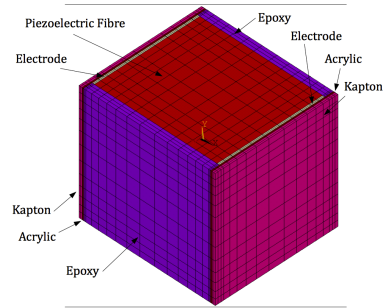


Figure 5. Finite element mesh for the 7-layered d_{15} MFC RVE with FVF=0.86.

Table 3 shows the effective properties, transformed to Voigt notation, of the d_{15} MFC, active layer only (columns 1 and 3) and full 7-layer composite (columns 2 and 4), using FVF of 0.86 and 0.95 obtained by the finite element local problems. The effective electromechanical coupling coefficient of the RVE k_{15} is evaluated from the effective elastic, piezoelectric and dielectric properties, c_{55}^E , d_{15} and ϵ_{11}^T , using (2). The results for the active layer only were validated in a previous work (Trindade and Benjeddou, 2010) through comparison with those obtained by analytical homogenization methods UFM (without the unidirectional electric field, UDEF, approximation) and AHM (with the UDEF approximation) Benjeddou and Al-Ajmi (2009). Notice however that, in (Trindade and Benjeddou, 2010), an equivalent homogeneous electrode layer (80% Copper, 20% Epoxy) was considered, which properties were evaluated using mixture laws, whereas, in the present case, the electrode layer is heterogeneous (Epoxy/Copper/Epoxy) and the Copper portion covers only the piezoceramic fibre, as shown in Figures 3b and 4. The present results are almost exactly the same as in (Trindade and Benjeddou, 2010).

The results show that the increase in the FVF from 0.86 to 0.95, meaning a 10% increase, leads to an overall increase in the elastic (stiffness) constants. More importantly, the effective piezoelectric properties of major interest to the d_{15} MFC, d_{15} or e_{15} , increase substantially by 10% and 123%, respectively, for the active layer. This yields an increase in the effective squared electromechanical coupling coefficient k_{15}^2 by 123%, from 10% to 23%, for the active layer.

Table 3 also shows that, while the active layer is almost transversally isotropic, the 7-layered composite is definitely orthotropic. In particular, the Young modulus Y_1 is significantly diminished due to the relatively soft protective layers. On the other hand, the Young modulus Y_3 is increased mainly due to the electrode that is stiffer than the Epoxy core and thus promotes a stiffer connection between the X_3^+ surface and the PZT core. The shear modulus G_{13} is diminished by 27% (for FVF 0.86) and 46% (for FVF 0.95) due to the protective layers which are softer than the PZT. Notice however that the thickness of the protective and electrode layers should also play a major role in this shear modulus, for instance a decrease on the thickness of these layers should increase the shear modulus G_{13} but will also perform poorly as protective layers. The piezoelectric constant d_{15} is increased a little while e_{15} is decreased by 30%, from 3.13 to 2.06 C/m². The dielectric constant ϵ_{11}^T is not modified due to the protective and electrode layers since it is assumed that the electric contact between electrode and PZT occurs at the PZT-electrode interface. This would not be the case if there should be an epoxy layer between Copper electrode and PZT. These effective properties yields an overall smaller electromechanical coupling coefficient k_{15} , such that the efficiency in energy conversion k_{15}^2 decreases by 20%, from 10% to 8%. Notice that this is much less than the k_{15}^2 of the PZT (Sonox P502) alone of 54.8%.

Table 3. Effective short-circuit material properties of d_{15} MFC and its active layer for two fibre volume fractions.

FVF=0.86		FVF=0.95	
MFC active layer	7-layers MFC	MFC active layer	7-layers MFC
$Y_1 = 50.12$ GPa	$Y_1 = 26.44$ GPa	$Y_1 = 54.90$ GPa	$Y_1 = 28.75$ GPa
$Y_2 = 50.12$ GPa	$Y_2 = 48.47$ GPa	$Y_2 = 54.90$ GPa	$Y_2 = 53.09$ GPa
$Y_3 = 20.55$ GPa	$Y_3 = 19.86$ GPa	$Y_3 = 37.63$ GPa	$Y_3 = 35.90$ GPa
$G_{23} = 6.88$ GPa	$G_{23} = 6.70$ GPa	$G_{23} = 15.03$ GPa	$G_{23} = 14.38$ GPa
$G_{13} = 6.49$ GPa	$G_{13} = 4.73$ GPa	$G_{13} = 13.09$ GPa	$G_{13} = 7.09$ GPa
$G_{12} = 16.60$ GPa	$G_{12} = 7.64$ GPa	$G_{12} = 18.22$ GPa	$G_{12} = 8.16$ GPa
$\nu_{12} = 0.43$	$\nu_{12} = 0.23$	$\nu_{12} = 0.43$	$\nu_{12} = 0.23$
$\nu_{13} = 0.20$	$\nu_{13} = 0.15$	$\nu_{13} = 0.20$	$\nu_{13} = 0.13$
$\nu_{23} = 0.20$	$\nu_{23} = 0.21$	$\nu_{23} = 0.20$	$\nu_{23} = 0.22$
$d_{15} = 486.67$ pC/N	$d_{15} = 485.60$ pC/N	$d_{15} = 532.61$ pC/N	$d_{15} = 532.60$ pC/N
$e_{15} = 3.13$ C/m ²	$e_{15} = 2.06$ C/m ²	$e_{15} = 6.97$ C/m ²	$e_{15} = 3.40$ C/m ²
$\epsilon_{11}^T = 15.01$ nF/m	$\epsilon_{11}^T = 14.95$ nF/m	$\epsilon_{11}^T = 16.42$ nF/m	$\epsilon_{11}^T = 16.41$ nF/m
$k_{15}^2 = 10.2$ %	$k_{15}^2 = 7.5$ %	$k_{15}^2 = 22.6$ %	$k_{15}^2 = 12.2$ %
$k_{15} = 32$ %	$k_{15} = 27$ %	$k_{15} = 48$ %	$k_{15} = 35$ %

6. PARAMETRIC ANALYSIS

In this section, a parametric analysis of the d_{15} MFC effective material properties is performed. The active layer fibre volume fraction, the Epoxy elastic modulus and the Copper electrode thickness are varied and the effect of these variations on the effective material properties are analyzed.

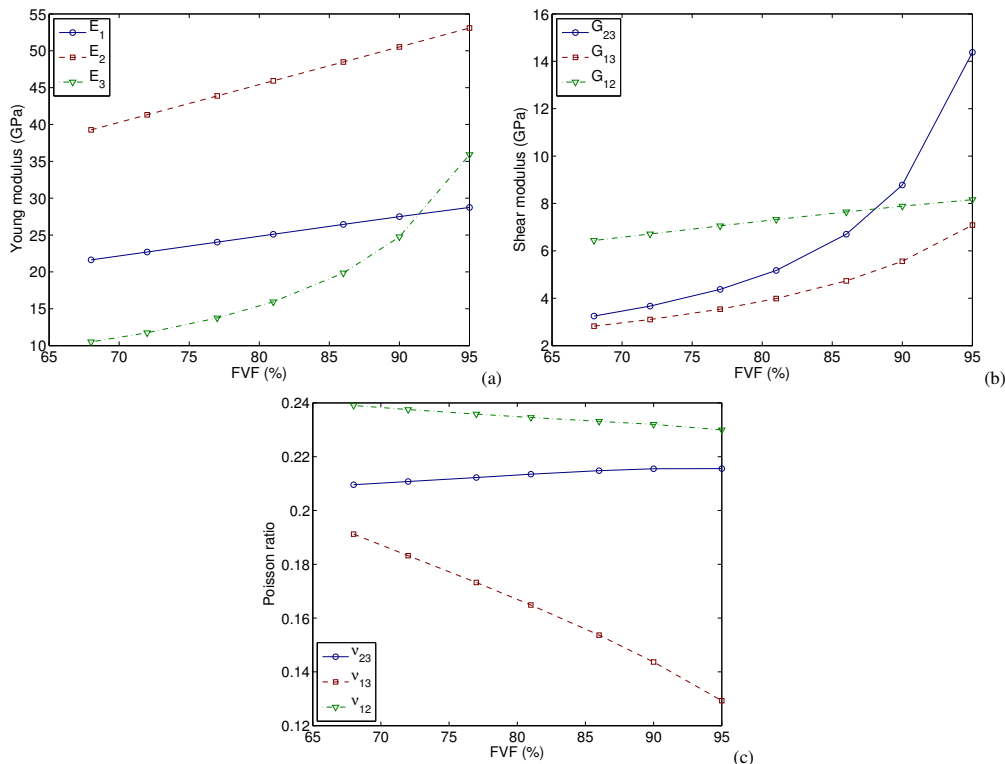


Figure 6. Variation of elastic material properties of d_{15} MFC with the active layer fibre volume fraction.

In a first analysis, the fibre volume fraction is varied in the range from 68% to 95%. Notice that the standard piezoelectric MFC are manufactured using a 86% FVF. As expected, all elastic stiffness coefficients increase for higher FVF since the piezoceramic is much stiffer than the Epoxy. A more detailed analysis shows however that whereas constants E_1 , E_2 and G_{12} increase linearly with the FVF, the other elastic stiffness constants E_3 , G_{23} and G_{13} present a non-linear augmentation, as shown in Figure 6. On the other hand, the Poisson ratios ν_{13} and ν_{12} decrease with increasing FVF and ν_{23} increases moderately. As shown in Figure 7, the piezoelectric and dielectric material properties increase substantially for higher FVF, since those are only due to the piezoelectric part of the active layer. It can be observed from Figure 7 that ϵ_{11}^T and d_{15} , dielectric and piezoelectric, constants increase linearly with FVF, while piezoelectric constant e_{15} and

squared electromechanical coupling coefficient k_{15}^2 increase rates augment with FVF, indicating that maximization of FVF is more important for applications using the d_{15} MFC as actuators or energy converters.

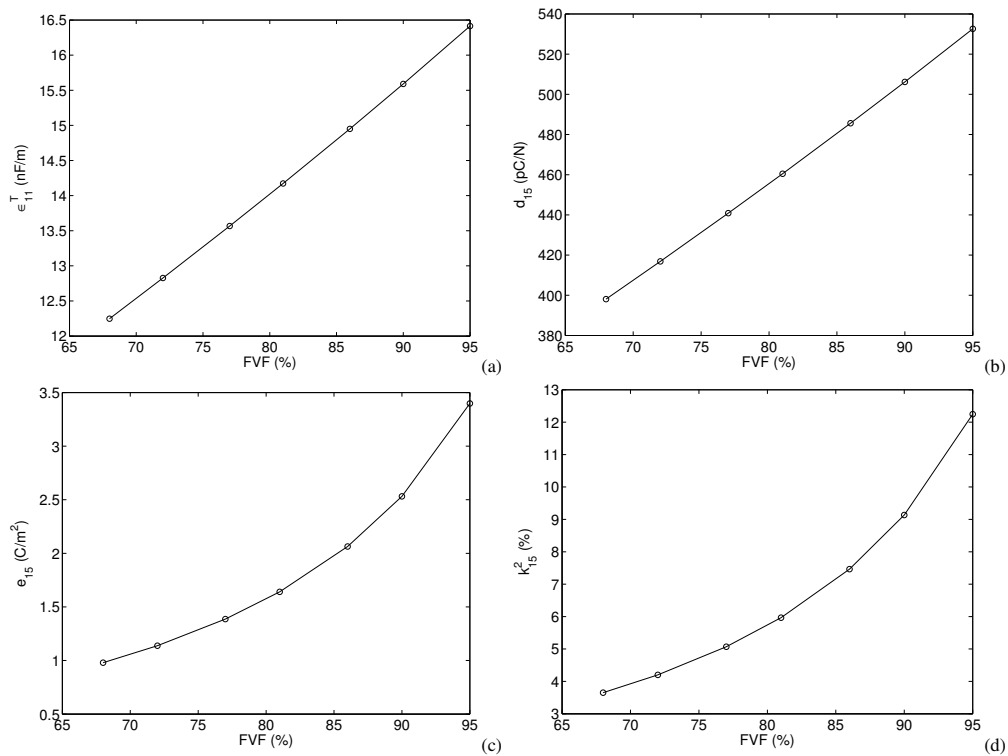


Figure 7. Variation of dielectric, piezoelectric and electromechanical coupling material properties of d_{15} MFC with the active layer fibre volume fraction.

In a second analysis, the effect of the Epoxy elastic modulus on the effective material properties is analyzed. Since the major part of elastic strains is concentrated in the Epoxy material, it is expected that stiffer Epoxy materials could improve both overall stiffness and electromechanical coupling. Indeed, as shown in Figure 8a, an increase of 20% on the Epoxy elastic modulus leads to an increase of almost 15% on d_{15} MFC elastic constant E_3 . On the other hand, effective elastic constants E_1 and E_2 are not significantly altered by the Epoxy elastic modulus. As for the shear elastic constants, G_{23} and G_{13} increase by around 15% and 10%, respectively, when Epoxy elastic modulus is increased by 20% while constant G_{12} remains nearly unchanged (Figure 8b). The Poisson ratios vary by less than 4% and, thus, are not shown in Figure 8.

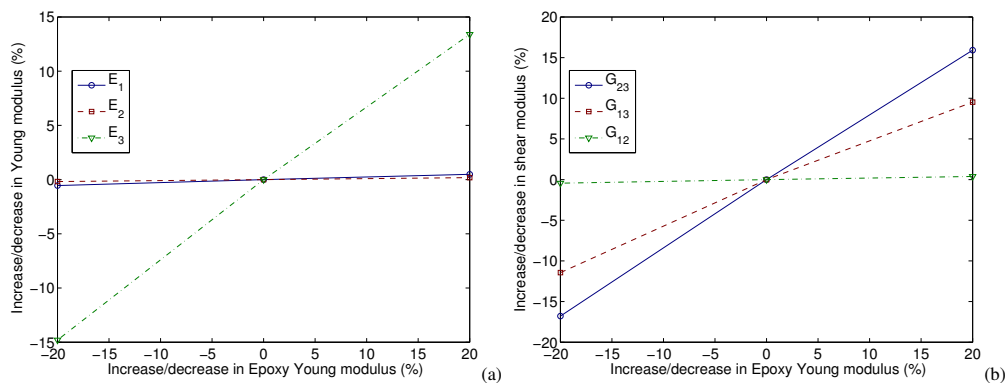


Figure 8. Variation of elastic material properties of d_{15} MFC with Epoxy elastic modulus.

On the other hand, the dielectric constant ϵ_{11}^T of the d_{15} MFC is not affected by the variation of Epoxy elastic modulus. The same happens to piezoelectric constant d_{15} . However, the piezoelectric constant e_{15} , which depends on the effective shear stiffness of the composite, increases approximately by 10% when the Epoxy elastic modulus is increased by 20%, as shown in Figure 9a. A very similar dependence is observed for the squared electromechanical coupling coefficient k_{15}^2 , shown in Figure 9b. This indicates that stiffer Epoxy materials should be more interesting for actuators and energy converters applications. Notice, however, that this would also lead to a less flexible (conformable) transducer.

From previous analyses, it seemed that electrode thickness could affect effective material properties of the d_{15} MFC,

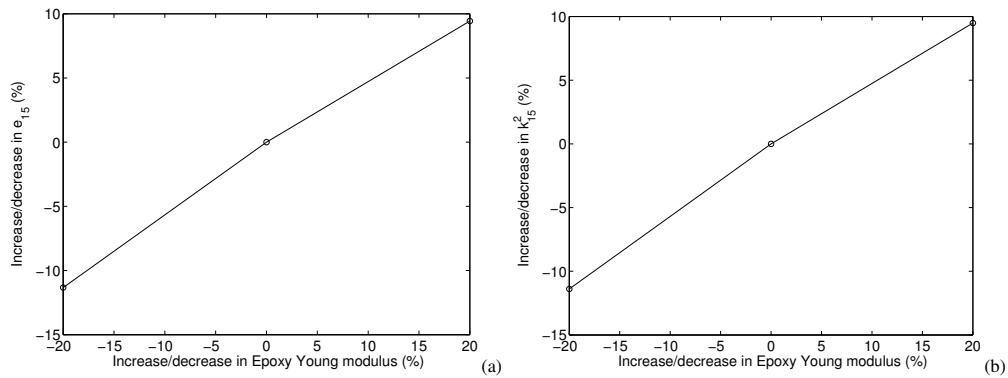


Figure 9. Variation of piezoelectric and electromechanical coupling material properties of d_{15} MFC with Epoxy elastic modulus.

since this layer responds to the major part of the covering layer (electrode and Kapton/Acrylic protective layers) stiffness. Therefore, this property was also varied by $\pm 20\%$. Since a Copper electrode is commonly used, it did not seem appropriate to vary its elastic modulus. For the same reason, the Kapton and Acrylic protective layers material properties were also kept unchanged. Figure 10 shows that an increase of the electrode thickness yields an overall augmentation of the d_{15} MFC stiffness constants, although this augmentation is smaller than 1%. Elastic constants E_1 , E_2 and G_{12} are the most affected by the electrode thickness variation. Poisson ratios (not shown) are not significantly affected. As for the variation of the previous parameter, dielectric constant ϵ_{11}^T and piezoelectric constant d_{15} are not affected by the variation of electrode thickness. On the other hand, the piezoelectric constant e_{15} decreases a little (0.4%), while the squared electromechanical coupling coefficient k_{15}^2 increases a little (0.2%), for an increase of 20% in the electrode thickness (Figure 11).

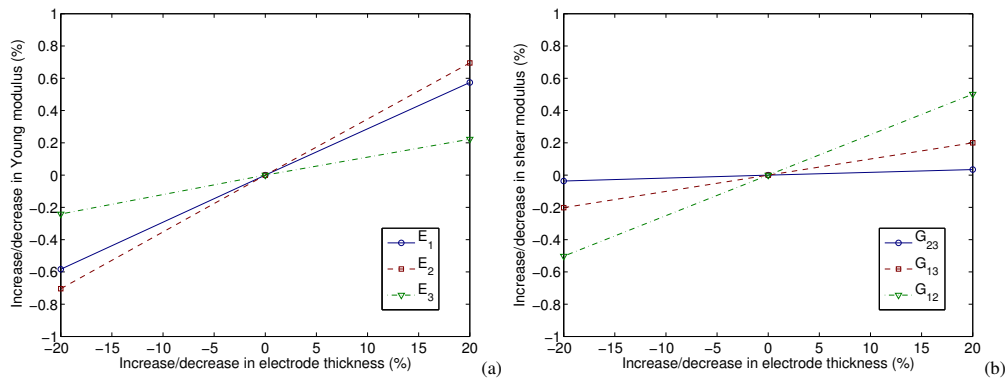


Figure 10. Variation of elastic material properties of d_{15} MFC with electrode thickness.

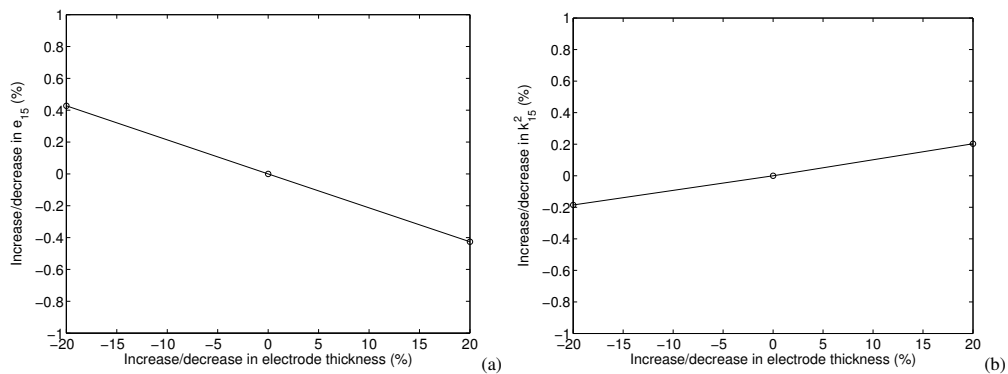


Figure 11. Variation of piezoelectric and electromechanical coupling material properties of d_{15} MFC with electrode thickness.

7. CONCLUDING REMARKS

In the present work, a finite element homogenization method for a shear actuated d_{15} Macro-Fibre Composite (MFC) made of seven layers (Kapton, Acrylic, Electrode, Piezoceramic Fibre and Epoxy Composite, Electrode, Acrylic, Kapton)

was proposed and used for the characterization and identification of its effective material properties. It was shown that the packaging reduces significantly the shear stiffness of the piezoceramic material and, thus, leading to significantly smaller effective electromechanical coupling coefficient k_{15} and piezoelectric stress constant e_{15} when compared to the piezoceramic fibre properties. However, the piezoelectric charge constant d_{15} was less affected by the softer layers required by the MFC packaging. This might indicate that this MFC design could be interesting for sensing applications but not so much for actuation. The presented results also confirmed that a higher fibre volume fraction (FVF) is desirable and a 95% FVF seems to be a good compromise. A parametric analysis for which fibre volume fraction, Epoxy elastic modulus and electrode thickness are varied was also performed and its results have shown that both fibre volume fraction and Epoxy elastic modulus affect significantly the electromechanical coupling coefficient of the proposed MFC and, thus, its performance as sensor, actuator and energy converter. On the other hand, the piezoelectric charge constant d_{15} and the dielectric constant ϵ_{11}^T were not significantly affected by variations of Epoxy elastic modulus and electrode thickness.

8. ACKNOWLEDGEMENTS

The authors acknowledge the support of the MCT/CNPq/FAPEMIG National Institute of Science and Technology on Smart Structures in Engineering, grant no.574001/2008-5.

9. REFERENCES

- Wilkie W K, Bryant G R and High J W 2000 Low-cost piezocomposite actuator for structural control applications *Proceedings of SPIE International Symposium on Smart Structures and Materials* (Newport Beach) 5-9 March
- Bent A A and Hagood N W 1997 Piezoelectric fiber composites with interdigitated electrodes *Journal of Intelligent Material Systems and Structures* **8** 903-919
- Raja S and Ikeda T 2008 Concept and electro-elastic modeling of shear actuated fiber composite using micro-mechanics approach *Journal of Intelligent Material Systems and Structures* **19** 1173-1183
- Benjeddou A 2007 Shear-mode piezoceramic advanced materials and structures: A state of the art *Mechanics of Advanced Materials and Structures* **14**(4) 263-275
- Trindade M A and Benjeddou A 2009 Effective electromechanical coupling coefficients of piezoelectric adaptive structures: critical evaluation and optimization *Mechanics of Advanced Materials and Structures* **16**(3) 210-223
- Raja S, Prathap G and Sinha P K 2002 Active vibration control of composite sandwich beams with piezoelectric extension-bending and shear actuators *Smart Materials and Structures* **11**(1) 63-71
- Baillargeon B P and Vel S S 2005 Exact solution for the vibration and active damping of composite plates with piezoelectric shear actuators *Journal of Sound and Vibration* **282** 781-804
- Benjeddou A and Ranger J-A 2006 Use of shunted shear-mode piezoceramics for structural vibration passive damping *Computers and Structures* **84** 1415-1425
- Trindade M A and Maio C E B 2008 Multimodal passive vibration control of sandwich beams with shunted shear piezoelectric materials *Smart Materials and Structures* **17** art.no.055015
- Deraemaeker A, Nasser H, Benjeddou A and Preumont A 2009 Mixing rules for the piezoelectric properties of macro fiber composites *Journal of Intelligent Material Systems and Structures* **20**(12) 1475-1482
- Benjeddou A and Al-Ajmi M 2009 Analytical homogenizations of piezoceramic d_{15} shear macro-fibre composites *Proceedings of the IUTAM Conference on Multiscale Modelling of Fatigue, Damage and Fracture in Smart Materials* ed M Kuna and A Ricoeur (Freiburg, Germany) Sept 1-4
- Otero J A, Rodriguez-Ramos R, Monsivais G and Pérez-Alvarez R 2005 Dynamical behavior of a layered piezocomposite using the asymptotic homogenization method *Mechanics of Materials* **37** 33-44
- Berger H, Kari S, Gabbert U, Rodriguez-Ramos R, Guinovart R, Otero J A and Bravo-Castirello J 2005 An analytical and numerical approach for calculating effective material coefficients of piezoelectric fiber composites *International Journal of Solids and Structures* **42** 5692-5714
- Trindade M A and Benjeddou A 2010 Modelling and characterization of shear actuated piezoelectric fibre composites *Proceedings of the Tenth International Conference on Computational Structures Technology* ed B H V Topping, J M Adam, F J Pallarés, R Bru and M L Romero (Stirlingshire: Civil-Comp Press) Valencia (Spain) paper 69
- Ikeda T 1990 Fundamentals of Piezoelectricity (Oxford University Press)
- Deraemaeker A, Benelechi S, Benjeddou A and Preumont A 2007 Analytical and numerical computation of homogenized properties of MFCs: Application to a composite boom with MFC actuators and sensors *III ECCOMAS Thematic Conference on Smart Structures and Materials* ed W Ostachowicz et al. (Gdansk, Poland) July 9-11

10. RESPONSIBILITY NOTICE

The authors are the only responsible for the printed material included in this paper.